Sex Chromosome Heteromorphism and the Fast-X Effect in Poeciliids

Iulia Darolti[1], Lydia J. M. Fong[1], Judith E. Mank[1,2]

1 Department of Zoology and Biodiversity Research Centre, University of British Columbia, Vancouver, Canada

2 Centre for Ecology and Conservation, College of Life and Environmental Sciences, University of Exeter, Cornwall, United Kingdom

Corresponding author: Iulia Darolti, e-mail: darolti@zoology.ubc.ca

Abstract

An accelerated rate of sequence evolution on the X chromosome compared to autosomes, known as Fast-X evolution, has been observed in a range of heteromorphic sex chromosomes. However, it remains unclear how early in the process of sex chromosome differentiation the Fast-X effect becomes detectible. Recently, we uncovered an extreme variation in sex chromosome heteromorphism across Poeciliid fish species. The common guppy, *Poecilia reticulata*, Endler's guppy, *P. wingei*, and the swamp guppy, *P. picta*, appear to share the same XY system and exhibit a remarkable range of heteromorphism. The sex chromosome system is absent in recent outgroups, including *P. latipinna* and *Gambusia holbrooki*. We combined analyses of sequence divergence and polymorphism data across Poeciliids to investigate X chromosome evolution as a function of hemizygosity and reveal the causes for Fast-X effects. Consistent with the extent of Y degeneration in each species, we detect higher rates of divergence on the X relative to autosomes and a strong Fast-X effect in *P. picta*, while no change in the rate of evolution of X-linked relative to autosomal genes in *P. reticulata*. In *P. wingei*, the species with intermediate sex chromosome differentiation, we see an increase in the rate of nonsynonymous substitutions on the older stratum of divergence only. We also use our comparative approach to test different models for the origin of the sex chromosomes in this clade. Taken together, our study reveals an important role of hemizygosity in Fast-X and suggests a single, recent origin of the sex chromosome system in this clade.

Keywords: sex chromosome evolution, heteromorphy, hemizygosity

Introduction

Owing to their unusual inheritance pattern and hemizygosity in males, X chromosomes display many distinct evolutionary properties compared to the rest of the genome (Charlesworth et al. 1987; Vicoso and Charlesworth 2006). The strength of selection and genetic drift, as well as the role of dominance and effective population size, are expected to differ between sex chromosomes and autosomes (Kirkpatrick and Hall 2004; Mank et al. 2010; Meisel and Connallon 2013). Comparing differences in the evolution of sex-linked and autosomal loci is important for understanding patterns of mutation and selection acting across the genome.

An elevated rate of coding sequence evolution on the X chromosome relative to the autosomes, referred to as the Fast-X effect (or Fast-Z in the case of ZW systems) has been observed in a diversity of organisms, including humans (Lu and Wu 2005), primates (Stevenson et al. 2007), mice (Kousathanas et al. 2014), birds (Mank et al. 2007; Mank et al. 2010; Wright et al. 2015), *Drosophila* (Mank et al. 2010; Ávila et al. 2014; Charlesworth et al. 2018), aphids (Jaquiéry et al. 2018), spiders (Bechsgaard et al. 2019), and lepidoptera (Pinharanda et al., 2019; Sackton et al., 2014). However, the magnitude of this effect can vary substantially across species due to demographic factors, differences in mating system or regulatory mechanisms acting on the sex chromosomes (Mank et al. 2010). Notably, all the cases of Fast-X above were observed in highly heteromorphic sex chromosomes, where very few genes, if any, remain on the Y chromosome and the X is largely hemizygous in the heterogametic sex.

There are two potential causes of Fast-X. The single functional copy of the X chromosome in males leads to hemizygous exposure of genes and therefore stronger purifying selection against recessive deleterious mutations and positive selection for recessive beneficial ones expressed in males (Charlesworth et al. 1987). This adaptive cause of Fast-X is mainly expected in species with heteromorphic sex chromosomes and highly degenerated Y chromosomes, as a large proportion of X-linked genes will be hemizygous in males. Alternatively, in every male and female pair, there are only three X chromosomes to four copies of each autosome, and this varies substantially based on mating system and type of heterogamety (Vicoso and Charlesworth 2009; Mank et al. 2010; Wright and Mank 2013; Wright et al. 2015). This reduced effective population size of the X relative to the autosomes diminishes the relative power of selection on the X, potentially leading to both greater genetic drift and fixation of weakly

deleterious mutations on the X chromosome (Charlesworth et al. 1987). This non-adaptive cause of Fast-X does not necessarily require male hemizygosity, just recombination suppression between the X and Y chromosomes and differences in effective population size between X-linked and autosomal loci, and could apply to X loci where the Y copy is expressed and remains functional.

Recently, we uncovered an extreme variation across Poeciliids in the rate of sex chromosome degeneration and dosage compensation. The same chromosome pair acts as the XY system in the common guppy, *Poecilia reticulata*, its sister species Endler's guppy, *P. wingei*, and the more distantly related swamp guppy, *P. picta,* all of which last shared a common ancestor roughly 20 million years ago (Darolti et al. 2019). Notably, *P. latipinna* and *G. holbrooki*, recent outgroup species to this clade, do not show evidence of a sex chromosome system on the same chromosome (Darolti et al. 2019), and therefore we hypothesized based on parsimony that the sex chromosome system arose roughly 20 mya (supplementary Fig. S1, Parsimony Model). Since this origin, the sex chromosomes of *P. reticulata* and *P. wingei* have remained largely homomorphic, with little sequence differentiation between the X and the Y. In contrast, the *P. picta* sex chromosomes are completely nonrecombining (with the exception of a small pseudoautosomal region at the distal end, >20 Mb) and the Y chromosome has undergone substantial degeneration, leaving most of the X chromosome in males effectively hemizygous (Darolti et al. 2019). Moreover, *P. picta* exhibits complete dosage compensation, a pattern that has also been observed in its sister taxon, *P. parae* (Metzger et al. 2021; Sandkam et al. 2021), which is predicted to accentuate the Fast-X effect (Charlesworth et al. 1987; Mank et al. 2010). The range of sex chromosome differentiation present in this clade allows us to investigate patterns of X chromosome coding sequence evolution and to test causes underlying Fast-X effects.

In contrast to the Parsimony Model, it has recently been proposed that the sex chromosomes of *P. reticulata* represent a recent turnover event, and that the highly diverged *P. picta* and *P. parae* system is in fact ancient (Charlesworth et al. 2021). This Turnover Model (supplementary Fig. S1) posits that the *P. picta* X chromosome arose well before the immediate ancestor of *P. parae, P. picta*, *P. reticulata* and *P. wingei*, and slowly diverged over time resulting in the heteromorphism observed. This model supposes that the homomorphism observed in *P. reticulata* and *P. wingei* represents a turnover event, where

89 the current guppy X and Y chromosomes arose from the ancestral X of *P. picta*. Sex
90 chromosome turnovers are frequent in many animal groups (Bachtrog et al. 2014), so the
91 model is plausible.

92 However, the unique molecular and evolutionary signatures that accumulate on sex
93 chromosomes remain observable even when they revert to being autosomes (Vicoso and
94 Bachtrog 2013). That means that if the Turnover Model is true, Fast-X patterns, evolving over
95 long periods of time in the distant ancestor of *P. picta*, would also remain detectible on the X
96 chromosome in *P. reticulata* and *P. wingei* after turnover. Furthermore, the Turnover Model
97 requires additional turnover events in several other taxa within the clade that do not share
98 the same sex chromosome as *P. picta* (supplementary Fig. S1), and we would also expect these
99 species to exhibit ancient patterns of Fast-X on the chromosome, which is fully autosomal.
100 Our comparative dataset allows us to also test these alternative hypotheses for the origin of
101 the guppy sex chromosomes.

102 Using a combination of sequence divergence, polymorphism and expression data analyses
103 across Poeciliid species, we estimate rates of gene sequence evolution across the genome and
104 assess the presence of Fast-X evolution in each system. Consistent with the extent of Y
105 degeneration, we find significantly higher rates of X coding sequence evolution compared to
106 the autosomes and a strong signal of Fast-X effect in *P. picta*, potentially accelerated by the
107 evolution of chromosome wide dosage compensation in this system. The absence of a
108 consistent Fast-X evolution in *P. reticulata* and *P. wingei*, as well as in the outgroup species *P.*
109 *latipinna* and *G. holbrooki*, argues against the Turnover Model.

110 **Results**

111 **Strong signal of Fast-X evolution in the heteromorphic sex chromosomes of *P. picta***

112 We first assessed the strength of Fast-X in our study species with heteromorphic sex
113 chromosomes. The extensive X chromosome hemizygosity of *P. picta* males is expected to
114 accentuate the strength of Fast-X evolution in this species (Vicoso and Charlesworth 2006), as
115 is the mechanism of complete X chromosome dosage compensation (Mank et al. 2010).
116 Indeed, our analysis in *P. picta* revealed a greater mutation rate on the X chromosome,
117 excluding genes in the pseudoautosomal region (PAR) (see methods), compared to the
118 autosomes, as shown through the significantly higher rate of nonsynonymous substitutions

119 for X-linked loci (1,000 replicates permutation test, $p < 0.001$; supplementary Table S1). *P.*
120 *picta* also exhibits a significantly elevated rate of divergence (d_N/d_S) on the X chromosome
121 relative to the rest of the genome (Fig. 1C) and a strong Fast-X effect (Fig. 2), calculated as the
122 ratio of the rate of nonsynonymous over synonymous substitutions for the X chromosome
123 relative to that for the autosomes.

124 **Absence of Fast-X effect in species with homomorphic sex chromosomes**

125 We next asked whether patterns of coding sequence evolution are different between *P. picta*
126 and the species with homomorphic sex chromosomes, *P. reticulata* and *P. wingei*. Previous
127 work has indicated that *P. reticulata* and *P. wingei* share the same male-heterogametic sex
128 chromosome system (Nanda et al. 2014; Morris et al. 2018; Darolti et al. 2019). Analyses of
129 coverage differences between males and females indicate that Y degeneration is restricted to
130 the distal end of the sex chromosomes, in a region ancestral to *P. reticulata* and *P. wingei*
131 (designated as Stratum I) (Wright et al. 2017; Darolti et al. 2019; Darolti et al. 2020; Fraser et
132 al. 2020), and suggest that Y degeneration is slightly more exaggerated in *P. wingei* compared
133 to *P. reticulata*. This nonrecombining region coincides with the previously mapped location of
134 the sex determining region in *P. reticulata* (Winge 1922; Winge 1927; Winge and Ditlevsen
135 1947; Traut and Winking 2001; Tripathi et al. 2009) and is also found across six natural guppy
136 populations (Almeida et al. 2021).

137 We therefore assessed the signal of Fast-X for genes in Stratum I (20-26Mb on *P. reticulata*
138 chromosome 12; 17-20Mb on *P. wingei* syntenic chromosome to guppy sex chromosome). In
139 *P. reticulata*, the rate of divergence for X-linked genes in Stratum I was not significantly
140 different than that for autosomal genes (Fig. 1A; supplementary Table S1). To exclude the
141 possibility that we were lacking power in our analysis due to the small number of genes
142 identified in Stratum I, we redid the analysis for *P. reticulata* using Ensembl coding sequences
143 instead of our *de novo* generated transcripts. We were able to recover more than twice as
144 many X-linked loci, however the estimates of divergence remain the same as those based on
145 *de novo* transcripts (supplementary Fig. S2).

146 In *P. wingei*, genes in Stratum I show significantly higher rates of nonsynonymous and of
147 synonymous substitutions (supplementary Table S1), however the overall rate of divergence
148 is similar between the autosomes and Stratum I (Fig. 1B) and the Fast-X effect is not as

149 accentuated as in *P. picta* (Fig. 2). Recent work has suggested that the *P. wingei* X and Y
150 chromosomes are somewhat more differentiated from each other compared to those of *P.*
151 *reticulata* (Darolti et al. 2019), and there is also evidence for this from previous cytogenetic
152 work (Nanda et al. 1992; Nanda et al. 2014). This greater divergence might explain the
153 difference in d_N/d_S estimates for X-linked genes in Stratum I that we observe between these
154 two species, though the effect is negligible. However, note that following filtering (see
155 methods), only a handful of *P. wingei* genes remained in Stratum I, and as such our statistical
156 power to detect a significant Fast-X signal in this species is reduced.

157 If the guppy sex chromosomes represent a turnover event, we would expect the pattern of
158 Fast-X in *P. picta* to still be observed throughout the *P. reticulata* and *P. wingei* sex
159 chromosomes outside of Stratum I, as the majority of it accumulated prior to turnover. Thus,
160 we next estimated rates of sequence divergence for the remainder of the X chromosome,
161 excluding genes in Stratum I and genes on the PAR (see methods), as the high recombination
162 events in the PAR can alter rates of evolution and polymorphism (Otto et al. 2011). The rate
163 of mutation and mean d_N/d_S on the X chromosome were not different from that on the
164 autosomes in either *P. reticulata* or *P. wingei* (Fig. 1A, B; Fig. 2; supplementary Table S1). This
165 finding is consistent with the limited Y degeneration observed in these species (Wright et al.
166 2017; Darolti et al. 2019), and contradicts the Turnover Model. In addition, the Turnover
167 Model also requires sex chromosome turnover events in the outgroup species to the *P.*
168 *reticulata–P. wingei* clade (supplementary Fig. S2). We therefore estimated sequence
169 divergence in the outgroups, *P. latipinna* and *G. holbrooki*, both species in which the guppy
170 chromosome 12 has not been implicated as the sex chromosome. Our data fails to show
171 elevated rates of evolution on the chromosome syntenic to the guppy X relative to the rest of
172 the genome in either *P. latipinna* or *G. holbrooki* (supplementary Table S1). This result,
173 together with our findings in *P. reticulata* and *P. wingei* argues against the Turnover Model.

174 Previous comparisons of replicate *P. reticulata* natural population have shown evidence for
175 greater X-Y divergence in replicate upstream, low predation populations relative to their
176 downstream, high predation populations pair within Quare, Aripo and Yarra rivers (Wright et
177 al. 2017; Almeida et al. 2021). This pattern of divergence has occurred over a relatively short
178 time span, at some point after the colonization of Trinidad at the last glacial maximum.
179 Therefore, we investigated whether we can detect higher rates of X chromosome to autosome

180 coding sequence evolution in upstream compared to downstream populations. We find a
181 significantly elevated d_N/d_S on the X chromosome, excluding genes on the PAR and those on
182 Stratum I, compared to the autosomes in the Yarra upstream population only (supplementary
183 Tables S2-4), and across all rivers we do not find a consistently stronger Fast-X effect in the
184 upstream relative to the downstream populations (Fig. 3). Compared to the other rivers, the
185 upstream population of the Yarra river shows the greatest increase in Y divergence relative to
186 the downstream population, measured by both male:female F_{ST} and male-specific SNPs
187 (Almeida et al. 2021). X-Y divergence between upstream and downstream populations is
188 greater in Yarra compared to Quare and Aripo, and this might explain why a pattern of Fast-X
189 effect in the upstream population is recovered in Yarra alone.

190 **Polymorphism and the underlying causes of Fast-X**

191 A higher d_N/d_S on the X chromosome relative to the rest of the genome could be the result of
192 both an increased genetic drift (Charlesworth et al. 1987; Mank et al. 2010) and an increased
193 efficacy of selection (Vicoso and Charlesworth 2009). Therefore, we used sequence and
194 polymorphism data together to test for the causes of elevated Fast-X evolution in *P. picta*. The
195 McDonald-Kreitman test contrasts the number of nonsynonymous and synonymous
196 substitutions with polymorphisms, where an excess of nonsynonymous substitutions relative
197 to polymorphisms is indicative of positive selection (McDonald and Kreitman 1991). Using this
198 test, we detected no X-linked genes with signatures of positive selection in any of the Poeciliid
199 species. However, the McDonald-Kreitman test is very conservative, as it is restricted to genes
200 with sufficient numbers of substitutions and polymorphisms (Begun et al. 2007; Andolfatto
201 2008), and as such our analysis was limited to a few X-linked contigs.

202 To increase our statistical power to detect signatures of positive selection, we also used the
203 direction of selection (DoS) test which is less sensitive to low cell counts (Stoletzki and Eyre-
204 Walker 2011). For each contig, DoS calculates the difference between the proportion of
205 nonsynonymous substitutions and the proportion of nonsynonymous polymorphisms, where
206 a positive DoS indicates adaptive evolution (Stoletzki and Eyre-Walker 2011). Using this
207 approach, we recovered more genes with signatures of positive selection, however the X
208 chromosome was not enriched in these genes compared to the rest of the genome in any of
209 the species (supplementary Table S6).

210 Next, we used polymorphism data alone to test for deviations from neutrality. A higher rate
211 of nonsynonymous to synonymous polymorphisms on the X relative to the autosomes is
212 indicative of reduced efficacy of selection to remove mildly deleterious mutations, while a
213 lower rate suggests purifying selection resulting from hemizygous exposure of deleterious
214 mutations in males. Our results show a lower, though not significantly, rate of nonsynonymous
215 polymorphisms in *P. picta* only (Table 1, supplementary Table S5), which may suggest that the
216 observed Fast-X effect in *P. picta* is influenced by purifying selection acting to remove
217 deleterious mutations on the X (Charlesworth et al. 1987; Vicoso and Charlesworth 2009).

218 **Discussion**

219 **The role of hemizygosity in Fast-X**

220 We observe a clear pattern of Fast-X in *P. picta*, as shown through the significantly higher rate
221 of nonsynonymous substitutions for X-linked loci (supplementary Table S1) and significantly
222 elevated rate of divergence on the X chromosome relative to the rest of the genome (Fig. 1C,
223 Fig. 2), consistent with the extensive Y chromosome degeneration in this species. In contrast,
224 we did not observe significant patterns of Fast-X evolution in either *P. reticulata* or *P. wingei*.
225 There is little evidence of loss of Y gene coding sequence in either of these species (Darolti et
226 al. 2019; Darolti et al. 2020), and very few, if any, genes are hemizygously expressed in males,
227 even in the older Stratum I. Interestingly, the *P. wingei* Y is somewhat more diverged than the
228 Y in *P. reticulata* (Nanda et al. 1992; Nanda et al. 2014; Darolti et al. 2019), and we observe a
229 slight, though non-significant Fast-X effect in Stratum I in the former. We also observe an
230 effect in the Yarra upstream population, which shows the greatest X-Y divergence across
231 natural populations in Trinidad (Almeida et al. 2021). All this points to the key role of sex
232 chromosome hemizygosity in driving Fast-X evolution.

233 Theory predicts that complete dosage compensation, whereby balance in expression between
234 the sex chromosomes and the autosomes is restored, may facilitate a more pronounced Fast-
235 X effect (Charlesworth et al. 1987; Mank et al. 2010). Under this theory, in systems with
236 incomplete dosage compensation, where only a subset of the genes is compensated for but
237 overall expression for X-linked genes is reduced compared to the autosomes in males, X-linked
238 beneficial mutations may have lower expression and weaker phenotypic effects in males,
239 potentially limiting the Fast-X effect (Charlesworth et al. 1987; Mank et al. 2010). *P. picta* has

240 evolved chromosome-wide dosage compensation, seemingly through a mechanism involving
241 the hyperexpression of the single X in males (Darolti et al. 2019), and this may have
242 contributed to the observed signature of Fast-X evolution.

243 There are two potential causes of Fast-X. Male heterogamety leads to hemizygous exposure
244 of genes and therefore stronger purifying selection against recessive deleterious mutations
245 and positive selection for recessive beneficial ones expressed in males (Charlesworth et al.
246 1987). Alternatively, the reduced effective population size of the X relative to the autosomes
247 diminishes the relative power of selection on the X, potentially leading to non-adaptive causes
248 of Fast-X (Charlesworth et al. 1987) which do not necessarily require male hemizygosity, just
249 recombination suppression between the X and Y chromosomes.

250 The role of hemizygosity and dosage compensation we observe in *P. picta* Fast-X suggest an
251 adaptive mechanism, and our polymorphism analysis is consistent with greater purifying
252 selection acting in males to remove recessive deleterious variation. However, although we
253 were unable to differentiate adaptive and non-adaptive causes of Fast-X in our polymorphism
254 data, polymorphism estimates are sensitive to demographic fluctuations (Tajima 1989; Pool
255 and Nielsen 2007) and, thus, it is difficult to determine to what extent the Fast-X pattern in *P.*
256 *picta* is adaptive using polymorphism data alone. Future work identifying true X-hemizygous
257 loci in males and analyzing their patterns of sequence evolution may prove more revealing.

258 **Differentiating different models of sex chromosome origin**

259 Two models have been proposed for the origin of the sex chromosome system in this group.
260 The Parsimony Model posits that the sex chromosomes arose roughly 20 mya (supplementary
261 Fig. S1) in the ancestor of the species that all share it and experienced different rates of Y
262 decay in different sub-clades (Darolti et al. 2019), possibly exacerbated by the evolution of
263 complete dosage compensation in *P. picta* and close relatives (Metzger et al. 2021; Sandkam
264 et al. 2021). The Turnover Model proposes that the sex chromosomes of *P. reticulata*
265 represent a recent turnover event, and that the highly diverged *P. picta* and *P. parae* system
266 arose well before the immediate ancestor of *P. parae, P. picta*, *P. reticulata* and *P. wingei*, and
267 slowly diverged over time resulting in the heteromorphism observed (Charlesworth et al.
268 2021). Because the molecular signatures that accumulate on sex chromosomes remain
269 observable even when they revert to being autosomes (Vicoso and Bachtrog 2013), we were

270 able to critically test these alternative models. If the guppy sex chromosomes represent a
271 turnover event, we would expect the pattern of Fast-X in *P. picta* to still be observed
272 throughout the *P. reticulata* and *P. wingei* sex chromosomes outside of Stratum I, as the
273 majority of it accumulated prior to turnover. In addition, the Turnover Model also requires sex
274 chromosome turnover events in the outgroup species to the *P. reticulata–P. wingei* clade, and
275 we would expect Fast-X in *P. latipinna* or *G. holbrooki*, where the ancient X chromosome is
276 presumably now fully autosomal.

277 We do not observe signatures of Fast-X in *P. reticulata* and *P. wingei* that would be consistent
278 with the Turnover Model, even after investigating multiple datasets (based on *de novo*
279 transcripts of a lab population and replicate wild populations, and Ensembl coding sequences).
280 Similarly, the lack of Fast-X in *P. latipinna* and *G. holbrooki*, the near outgroups to *P. picta, P.*
281 *reticulata,* and *P. wingei* (Darolti et al. 2019), which would have also experienced sex
282 chromosome turnover to alternative autosomes if the *P. picta* sex chromosomes are ancient,
283 also argues against an ancient origin and turnover. Instead, our results support the Parsimony
284 Model, and suggest that the sex chromosomes originated in the immediate ancestor of the *P.*
285 *picta–P. reticulata–P. wingei* clade and divergence occurred more rapidly in *P. picta,*
286 potentially accelerated by the evolution of complete X chromosome dosage compensation in
287 this species, which reduces selection to maintain Y chromosome expression for dosage
288 sensitive genes (Metzger et al. 2021).

289 Materials and Methods

290 Sample collection and sequencing

291 We have previously obtained tissue samples, extracted and sequenced RNA from the tails of
292 three males and three females of *P. reticulata*, *P. wingei*, *P. picta*, *P. latipinna* and *G. holbrooki*
293 (BioProject ID PRJNA353986, PRJNA528814) (Wright et al. 2017; Darolti et al. 2019). *P.*
294 *reticulata* samples were obtained from our outbred laboratory population originating from
295 the Quare River in Trinidad (Kotrschal et al. 2013). *P. wingei* samples were collected from our
296 laboratory population established from a strain maintained by a UK fish fancier. *P. picta*
297 samples were acquired from Guyana, while *P. latipinna* and *G. holbrooki* samples were
298 obtained in Florida. All samples were collected in accordance with national and institutional
299 ethical guidelines.

300 We extracted RNA from each sample using the Qiagen RNeasy Kit, following the instructions
301 of the manufacturer. Library preparation and sequencing were performed at the University
302 of Oxford Wellcome Centre for Human Genetics, following standard Illumina protocols and
303 using the Illumina HiSeq 4000 platform. The data were quality assessed using FastQC v0.11.3
304 (www.bioinformatics.babraham.ac.uk/projects/fastqc) and trimmed with Trimmomatic
305 v0.36 (Bolger 2014), removing adaptor sequences, reads with an average Phred score < 15 in
306 a sliding window of four bases, reads with leading or trailing bases with a Phred score < 3 and
307 reads shorter than 50bp following trimming.

308 **Identifying orthogroups**

309 For each species, we mapped RNA-seq reads to a previously constructed species-specific
310 female *de novo* genome assembly (Wright et al. 2017; Darolti et al. 2019) using HISAT2 v2.0.4
311 (Kim et al. 2015), with the exception of *P. latipinna* for which a male genome assembly was
312 used, and a non-redundant set of transcripts in GTF file format was constructed using
313 StringTie v1.2.4 (Pertea et al. 2015). We filtered the transcripts for non-coding RNA (ncRNA)
314 by extracting transcript sequences with BEDtools getfasta (Quinlan and Hall 2010) and
315 removing transcripts with a BLAST hit to ncRNA sequences from *Poecilia formosa*
316 (PoeFor_5.1.2), *Oryzias latipes* (MEDAKA1), *Gasterosteus aculeatus* (BROADS1) and *Danio*
317 *rerio* (GRCz10) from Ensembl 104 (Flicek et al. 2014). Only genes with positional information
318 on chromosomal fragments were kept for further analyses and the longest isoform for each
319 target gene was selected. Lastly, we applied a minimum expression filter of 2 RPKM in at least
320 half of the samples of each sex (minimum of two out of three individuals of either sex),
321 resulting in 13,306 *P. reticulata*, 15,089 *P. wingei,* 13,156 *P. picta*, 14,468 *P. latipinna* and
322 21,861 *G. holbrooki* genic sequences.

323 We obtained coding sequences from the outgroup species *P. formosa* (PoeFor_5.1.2),
324 *Xiphophorus maculatus* (Xipmac4.4.2) and *O. latipes* (MEDAKA1) from Ensembl 104 and
325 extracted the longest isoform for each gene. Separately for each of our target species, we
326 determined orthology across target and outgroup sequences using reciprocal BLASTn v2.7.1
327 (Altschul et al. 1990) with an e-value cut-off of $10e^{-10}$ and a minimum percentage identity of
328 30%. For genes with multiple blast hits, we chose the top hit based on the highest BLAST
329 score. Our analysis resulted in 7,296 *P. reticulata*, 7,253 *P. wingei*, 7,786 *P. picta*, 7,251 *P.*
330 *latipinna* and 6,477 *G. holbrooki* orthogroups (four-way 1:1 orthologs).

331 **Estimating sequence divergence across orthogroups**

332 For each contig of each orthogroup, we obtained open reading frames using *O. latipes*
333 (MEDAKA1) protein-coding sequences from Ensembl 104 and BLASTx v2.3.0 with an e-value
334 cut-off of $10e^{-10}$ and a minimum percentage identity of 30%, excluding orthogroups without
335 BLASTx hits or valid protein-coding sequences. We aligned orthologous gene sequences with
336 PRANK v170427 (Löytynoja and Goldman 2008), using the rooted tree (((Target species, *P.*
337 *formosa)*, *X. maculatus*), *O. latipes*), where the target species was in turn *P. reticulata*, *P.*
338 *wingei*, *P. picta*, *P. latipinna* and *G. holbrooki*. Alignments were then filtered to remove gaps.

339 To avoid false positive signals of adaptive evolution, poorly aligned or error-rich regions were
340 masked with SWAMP (Harrison et al. 2014). We ran SWAMP twice, first using a threshold of
341 six nonsynonymous substitutions in a window size of 15 codons, and second using a threshold
342 of two and a window size of five. This approach eliminates sequencing errors that cause short
343 stretches of nonsynonymous substitutions as well as alignment errors that cause longer
344 stretches of nonhomologous sequence due to variation in exon splicing or misannotation
345 (Harrison et al. 2014). To select these thresholds, we first applied a range of masking criteria
346 on our datasets. We then ran the branch-site test for positive selection on the target species
347 branches for both the unmasked and masked datasets. We visually inspected the alignments
348 of genes with the highest likelihood ratios and chose the masking criteria that was most
349 efficient at reducing false positive rates. Finally, we discarded orthologs for which the
350 alignment length was shorter than 300 bp following gap removal and masking, as these likely
351 represent incomplete sequences.

352 To obtain divergence estimates for each orthogroup and calculate mean d_N/d_S across the
353 target species branch, we used branch model (model=2, nssites=0) in the CODEML package
354 in PAML v4.8 (Yang 2007), using the phylogeny ((Target species#1, *P. formosa*), *X. maculatus*,
355 *O. latipes*), where the target species was successively *P. reticulata*, *P. wingei*, *P. picta*, *P.*
356 *latipinna* and *G. holbrooki*. To avoid inaccurate divergence estimates dues to mutational
357 saturation and double hits, orthologous genes with $d_S > 2$ were removed from subsequent
358 analyses (Axelsson et al. 2008).

359 For each of the target species, we divided orthologs into autosomal and sex-linked categories
360 based on their chromosomal location. The sex-linked category excluded genes in the

361 previously identified pseudoautosomal regions (0-5Mb and >26Mb of *P. reticulata*
362 chromosome 12; >20Mb of *P. wingei*, *P. picta*, *P. latipinna* and *G. holbrooki* chromosomes
363 that are syntenic to the guppy chromosome 12 (Darolti et al. 2019)). In addition, it has
364 recently been discovered that the *P. reticulata* reference genome, which served as reference
365 for scaffold ordering and orientation for our *P. reticulata* de novo genome assembly, has a
366 large inversion on the X chromosome that is specific to the guppy strain on which the
367 reference genome assembly was built and is not present in any of our lab or wild-caught
368 samples (Darolti et al. 2020; Almeida et al. 2021). We thus corrected for this inversion when
369 excluding genes from the PAR and assigning genes to the sex-linked category in *P. reticulata*.

370 Separately for each genomic category, we extracted the number of nonsynonymous
371 substitutions (D_N), the number of nonsynonymous sites (N), the number of synonymous
372 substitutions (D_S) and the number of synonymous sites (S). Taking into account alignment
373 length, we calculated mean d_N and mean d_S as the ratio of the number of substitutions across
374 all orthologs in that group divided by the number of sites ($d_N = D_N$ /N; $d_S = D_S$ /S), thus avoiding
375 bias from short sequences and the issue of infinitely high d_N/d_S estimates due to very low d_S
376 (Mank et al. 2007). We identified significant differences in d_N, d_S and d_N/d_S between genomic
377 categories using 1,000 permutation test replicates and we used bootstrapping with 1,000
378 replicates to determine 95% confidence intervals. The strength of the Faster-X effect was
379 calculated for each target species as the ratio of the rate of divergence for the X chromosome
380 over the rate of divergence for the autosomes X(d_N/d_S):A(d_N/d_S).

381 **Additional sequence divergence analyses for *P. reticulata***

382 For comparison to our estimates of rates of divergence based on *de novo* transcripts, we also
383 estimated rates of sequence evolution in *P. reticulata* using publicly available coding
384 sequences from Ensembl 104 (Guppy_female_1.0_MT). For this analysis, we followed the
385 same steps outlined above in terms of extracting the longest isoform for each gene,
386 identifying orthogroups, aligning target and outgroup sequences, masking and obtaining
387 divergence estimates.

388 In addition, we have previously constructed high quality *P. reticulata* female *de novo* genome
389 assemblies for replicate upstream and downstream populations of three rivers in Trinidad,
390 Quare, Aripo, and Yarra (Almeida et al. 2021). To each genome assembly, we mapped *P.*

391 *reticulata* RNA-seq reads from our laboratory population and generated a non-redundant set
392 of transcripts for each wild population following the methods detailed above. For each
393 upstream and downstream population, we then estimated rates of coding sequence
394 evolution for the X chromosome, excluding the PAR, and the autosomes by following the
395 same pipeline described in the previous section.

396 **Polymorphism data**

397 To obtain polymorphism data, for each target species we first mapped female RNA-seq reads
398 to the genome assembly using the STAR v2.4.2a aligner in two-pass mode (Dobin et al. 2013),
399 and then called SNPs using SAMtools v1.3.1 mpileup (Li et al. 2009) with a minimum base
400 quality of 20 and VarScan v2.3.9 mpileup2snp (Koboldt et al. 2012) with a minimum coverage
401 of two, a minimum average quality of 20, a minimum variant allele frequency of $1e^{-1}$, *p* value
402 of 0.05 and strand filter set to on. We next imposed that the polymorphism dataset also
403 passes the filtering criteria used for calculating rates of sequence divergence. As such, we
404 identified codons for which all sites pass the minimum coverage threshold of 20, there are no
405 alignment gaps following alignment with PRANK, and no ambiguity data (Ns) following
406 masking with SWAMP. To make our dataset compatible for the McDonald-Kreitman test of
407 selection, we only kept genes with both divergence and polymorphism data. Finally, for each
408 genomic category, we calculated mean p_N and mean p_S as the ratio of the number of
409 polymorphisms across all orthologs in that group divided by the number of sites (p_N=P_N/N;
410 p_S=P_S/N).

411 **Testing for selection using divergence and polymorphism data**

412 For each species, we estimated the number of genes evolving under neutral and adaptive
413 evolution using the McDonald-Kreitman test (McDonald and Kreitman 1991). Neutral theory
414 predicts that the ratio of nonsynonymous to synonymous changes within species (p_N/p_S)
415 should be equal to that between species (d_N/d_S) (McDonald and Kreitman 1991). As such, the
416 McDonald-Kreitman test identifies signatures of positive selection, where there is an excess
417 of nonsynonymous substitutions relative to polymorphisms ($d_N/d_S>p_N/p_S$), and of relaxed
418 purifying selection, where there is a deficit of nonsynonymous substitutions compared to
419 polymorphisms ($d_N/d_S<p_N/p_S$). To test for deviations from neutrality, for each contig, we used
420 a 2 x 2 contingency table and a Fisher's Exact Test in R v3.6.2 (R Core Team 2015). The power
421 of the McDonald-Kreitman test is limited with low table counts, therefore we restricted this

422 analysis to genes for which the sum of each row and column in the contingency table was
423 equal to or greater than six (Begun et al. 2007; Andolfatto 2008).

424 As the McDonald-Kreitman test is a very conservative test, we also used the divergence and
425 polymorphism data to calculate the direction of selection statistic (DoS) (Stoletzki and Eyre-
426 Walker 2011). For each gene, we calculated the difference between the proportion of
427 nonsynonymous substitutions and polymorphisms (DoS=$D_N(D_N+D_S)-P_N(P_N+P_S)$), where
428 positive DoS values are indicative of positive selection. We used Fisher's Exact test in R to test
429 for significant differences in the proportion of genes under positive selection between the
430 autosomes and the X chromosome in each species.

431 Lastly, we used the polymorphism data alone to test for an excess or deficit of
432 nonsynonymous polymorphisms on the X chromosome compared to the autosomes, which
433 would suggest a relaxed constraint or purifying selection, respectively. For this, we
434 concatenated P_N and P_S estimates within each species and used Fisher's Exact test in R to test
435 for significant differences in P_N/P_S between the autosomes and the X chromosome.

436 **Acknowledgements**

437 This work was supported by the European Research Council (grant agreement 680951), a
438 Canada 150 Research Chair, and an NSERC Discovery Grant to J.E.M. We thank C. Lacy for the
439 fish illustrations and members of the Mank lab for helpful discussions and suggestions.

440 **Author Contributions**

441 J.E.M. and I.D. designed the research; I.D. and L.F. performed the research; I.D., L.F. and J.E.M.
442 analyzed the data; I.D., L.F. and J.E.M. wrote the manuscript.

443 **References**

444 Almeida P, Sandkam BA, Morris J, Darolti I, Breden F, Mank JE. 2021. Divergence and
445 remarkable diversity of the Y chromosome in guppies. Mol Biol Evol. 38:619–633.

446 Altschul SF, Gish W, Miller W, Myers E, Lipman DJ. 1990. Basic local alignment search tool. J
447 Mol Biol. 215:403–410.

448 Andolfatto P. 2008. Controlling Type-I Error of the McDonald–Kreitman Test in Genomewide
449 Scans for Selection on Noncoding DNA. Genetics. 180:1767–1771.

450 Ávila V, De Procé SM, Campos JL, Borthwick H, Charlesworth B, Betancourt AJ. 2014. Faster-
451 X effects in two drosophila lineages. Genome Biol Evol. 6:2968–2982.

452 Axelsson E, Hultin-Rosenberg L, Brandström M, Zwahlén M, Clayton DF, Ellegren H. 2008.
453 Natural selection in avian protein-coding genes expressed in brain. Mol Ecol. 17:3008–3017.

454 Bachtrog D, Mank JE, Peichel CL, Kirkpatrick M, Otto SP, Ashman TL, Hahn MW, Kitano J,
455 Mayrose I, Ming R, et al. 2014. Sex determination: why so many ways of doing it? PLoS Biol.
456 12:e1001899.

457 Bechsgaard J, Schou MF, Vanthournout B, Hendrickx F, Knudsen B, Settepani V, Schierup
458 MH, Bilde T. 2019. Evidence for faster X chromosome evolution in spiders. Mol Biol Evol.
459 36:1281–1293.

460 Begun DJ, Holloway AK, Stevens K, Hillier LW, Poh YP, Hahn MW, Nista PM, Jones CD, Kern
461 AD, Dewey CN, et al. 2007. Population genomics: whole-genome analysis of polymorphism
462 and divergence in *Drosophila simulans*. PLoS Biol. 5:2534–2559.

463 Bolger AMLMUB. 2014. Trimmomatic: a flexible trimmer for Illumina sequence data.
464 Bioinformatics. 30:2114–2120.

465 Charlesworth B, Campos JL, Jackson BC. 2018. Theory and evidence from *Drosophila*. Mol
466 Ecol. 27:3753–3771.

467 Charlesworth B, Coyne JA, Barton NH. 1987. The relative rates of evolution of sex
468 chromosomes and autosomes. Am Nat. 130:113–146.

469 Charlesworth D, Bergero R, Graham C, Gardner J, Keegan H. 2021. How did the guppy Y
470 chromosome evolve? PLoS Genet. 17:e1009704.

471 Darolti I, Wright AE, Mank JE. 2020. Guppy Y chromosome integrity maintained by
472 incomplete recombination suppression. Genome Biol Evol. 12:965–977.

473 Darolti I, Wright AE, Sandkam BA, Morris J, Bloch NI, Farré M, Fuller RC, Bourne GR, Larkin
474 DM, Breden F, et al. 2019. Extreme heterogeneity in sex chromosome differentiation and
475 dosage compensation in livebearers. Proc Natl Acad Sci USA. 116:19031–19036.

476 Dobin A, Davis CA, Schlesinger F, Drenkow J, Zaleski C, Jha S, Batut P, Chaisson M, Gingeras
477 TR. 2013. STAR: ultrafast universal RNA-seq aligner. Bioinformatics. 29:15–21.

478 Flicek P, Amode MR, Barrell D, Beal K, Billis K, Brent S, …, Searle SMJ. 2014. Ensembl 2014.
479 Nucleic Acids Res. 42:749–755.

480 Fraser BA, Whiting JR, Paris JR, Weadick CJ, Parsons PJ, Charlesworth D, Bergero R, Bemm F,
481 Hoffmann M, Kottler VA, et al. 2020. Improved reference genome uncovers novel sex-linked
482 regions in the guppy (*Poecilia reticulata*). Genome Biol Evol. 12:1789–1805.

483 Harrison PW, Jordan GE, Montgomery SH. 2014. SWAMP : Sliding Window Alignment
484 Masker for PAML. Evol Bioinform. 10:EBO-S18193.

485 Jaquiéry J, Peccoud J, Ouisse T, Legeai F, Prunier-Leterme N, Gouin A, Nouhaud P, Brisson
486 JA., Bickel R, Purandare S, et al. 2018. Disentangling the Causes for Faster-X Evolution in
487 Aphids. Genome Biol Evol. 10:507–520.

488 Kim D, Langmead B, Salzberg SL. 2015. HISAT: A fast spliced aligner with low memory
489 requirements. Nat Methods. 12:357–360.

490 Kirkpatrick M, Hall DW. 2004. Male-biased mutation, sex linkage, and the rate of adaptive
491 evolution. Evol. 58:437–440.

492 Koboldt DC, Zhang Q, Larson DE, Shen D, McLellan MD, Lin L, Miller CA, Mardis ER, Ding L,
493 Wilson RK. 2012. VarScan 2: Somatic mutation and copy number alteration discovery in
494 cancer by exome sequencing. Genome Res. 22:568–576.

495 Kotrschal A, Rogell B, Bundsen A, Svensson B, Zajitschek S, Immler S, Maklakov AA, Kolm N.
496 2013. Experimental evidence for costs and benefits of evolving a larger brain. Curr Biol.
497 23:168–171.

498 Kousathanas A, Halligan DL, Keightley PD. 2014. Faster-X adaptive protein evolution in
499 house mice. Genetics. 196:1131–1143.

500 Li H, Handsaker B, Wysoker A, Fennell T, Ruan J, Homer N, Marth G, Abecasis G, Durbin R.
501 2009. The sequence alignment / map format and SAMtools. Bioinformatics. 25:2078–2079.

502 Löytynoja A, Goldman N. 2008. Phylogeny-aware gap replacement prevents errors in
503 sequence alignment and evolutionary analysis. Science. 320:1632–1635.

504 Lu J, Wu C-I. 2005. Weak selection revealed by the whole-genome comparison of the X
505 chromosome and autosomes of human and chimpanzee. PNAS. 102:4063–4067.

506 Mank JE, Axelsson E, Ellegren H. 2007. Fast-X on the Z: rapid evolution of sex-linked genes in
507 birds. Genome Res. 17:618–624.

508 Mank JE, Vicoso B, Berlin S, Charlesworth B. 2010. Effective population size and the Faster-X
509 effect: empirical results and their interpretation. Evolution. 64:663–674.

510 McDonald JH, Kreitman M. 1991. Adaptive protein evolution at the ADH locus in *Drosophila*.
511 Nature. 351:652–654.

512 Meisel RP, Connallon T. 2013. The faster-X effect: integrating theory and data. Trends
513 Genet. 29:537–544.

514 Metzger DCH, Sandkam BA, Darolti I, Mank JE. 2021. Rapid evolution of complete dosage
515 compensation in *Poecilia*. Genome Biol Evol. 13:evab155.

516 Morris J, Darolti I, Bloch NI, Wright AE, Mank JE. 2018. Shared and Species-Specific Patterns
517 of Nascent Y Chromosome Evolution in Two Guppy Species. Genes. 9:238.

518 Nanda I, Schartl M, Feichtinger W, Epplen JT, Schmid M. 1992. Early stags of sex
519 chromosome differentiation in fish as analysed by simple repetitive DNA sequences.
520 Chromosoma. 101:301–310.

521 Nanda I, Schories S, Tripathi N, Dreyer C, Haaf T, Schmid M, Schartl M. 2014. Sex
522 chromosome polymorphism in guppies. Chromosoma. 123:373–383.

523 Otto SP, Pannell JR, Peichel CL, Ashman T-L, Charlesworth D, Chippindale AK, Delph LF,
524 Guerrero RF, Scarpino S V, McAllister BF. 2011. About PAR: the distinct evolutionary
525 dynamics of the pseudoautosomal region. Trends Genet. 27:358–367.

526 Pertea M, Pertea GM, Antonescu CM, Chang TC, Mendell JT, Salzberg SL. 2015. StringTie
527 enables improved reconstruction of a transcriptome from RNA-seq reads. Nat Biotechnol.
528 33:290–295.

529 Pinharanda A, Rousselle M, Martin SH, Hanly JJ, Davey JW, Kumar S, Galtier N, Jiggins CD.
530 2019. Sexually dimorphic gene expression and transcriptome evolution provide mixed
531 evidence for a fast-Z effect in *Heliconius*. J Evol Biol. 32:194–204.

532 Pool JE, Nielsen R. 2007. Population size changes reshape genomic patterns of diversity. J
533 Org Evol. 61:30001–3006.

534 Quinlan AR, Hall IM. 2010. Genome analysis BEDTools: A flexible suite of utilities for
535 comparing genomic features. Bioinformatics. 26:841–842.

536 R Core Team. 2015. R: A language and environment for statistical computing. Vienna,
537 Austria: R Foundation for Statistical Computing. Available from: https//www.r-project.org.
538 Accessed August 25, 2021.

539 Rousselle M, Faivre N, Ballenghien M, Galtier N, Nabholz B. 2016. Hemizygosity enhances
540 purifying selection: Lack of fast-Z evolution in two satyrine butterflies. Genome Biol Evol.
541 8:3108–3119.

542 Sackton TB, Corbett-Detig RB, Nagaraju J, Vaishna L, Arunkumar KP, Hartl DL. 2014. Positive
543 selection drives faster-Z evolution in silkmoths. Evolution. 68:2331–2342.

544 Sandkam BA, Almeida P, Darolti I, Furman BLS, van der Bijl W, Morris J, Bourne GR, Breden
545 F, Mank JE. 2021. Extreme Y chromosome polymorphism corresponds to five male
546 reproductive morphs of a freshwater fish. Nat Ecol Evol. 5:939–948.

547 Stevenson BJ, Iseli C, Panji S, Zahn-Zabal M, Hide W, Old LJ, Simpson AJ, Jongeneel CV. 2007.
548 Rapid evolution of cancer/testis genes on the X chromosome. BMC Genomics. 8:1–11.

549 Stoletzki N, Eyre-Walker A. 2011. Estimation of the neutrality index. Mol Biol Evol. 28:63–70.

550 Tajima F. 1989. The effect of change in population size on DNA polymorphism. Genetics.
551 123:597–601.

552 Traut W, Winking H. 2001. Meiotic chromosomes and stages of sex chromosome evolution
553 in fish: zebrafish, platyfish and guppy. Chromosom Res. 9:659–672.

554 Tripathi N, Hoffmann M, Willing EM, Lanz C, Weigel D, Dreyer C. 2009. Genetic linkage map
555 of the guppy, *Poecilia reticulata*, and quantitative trait loci analysis of male size and colour
556 variation. Proc Biol Sci. 276:2195–2208.

557 Vicoso B, Bachtrog D. 2013. Reversal of an ancient sex chromosome to an autosome in
558 Drosophila. Nature. 499:332–335.

559 Vicoso B, Charlesworth B. 2006. Evolution on the X chromosome: unusual patterns and
560 processes. Nat Rev Genet. 7:645.

561 Vicoso B, Charlesworth B. 2009. The deficit of male-biased genes on the *D. melanogaster* X
562 chromosome is expression-dependent: A consequence of dosage compensation? J Mol Evol.
563 68:576–583.

564 Winge Ö. 1922. One-sided masculine and sex-linked inheritance in *Lebistes reticulatus*. J
565 Genet. 12:145–162.

566 Winge Ö. 1927. The location of eighteen genes in *Lebistes reticulatus*. J Genet. 18:1–43.

567 Winge Ö, Ditlevsen E. 1947. Colour inheritance and sex determination in *Lebistes*. Heredity.
568 1:65–83.

569 Wright AE, Darolti I, Bloch NI, Oostra V, Sandkam B, Buechel SD, Kolm N, Breden F, Vicoso B,
570 Mank JE. 2017. Convergent recombination suppression suggests role of sexual selection in

571 guppy sex chromosome formation. Nat Commun. 8:14251.

572 Wright AE, Harrison PW, Zimmer F, Montgomery SH, Pointer MA, Mank JE. 2015. Variation
573 in promiscuity and sexual selection drives avian rate of Faster-Z evolution. Mol Ecol.
574 24:1218–1235.

575 Wright AE, Mank JE. 2013. The scope and strength of sex-specific selection in genome
576 evolution. J Evol Biol. 26:1841–1853.

577 Yang Z. 2007. PAML 4: phylogenetic analysis by maximum likelihood. Mol Biol Evol.
578 24:1586–1591.

579

580 **Figure Legends**

581 **Figure 1. Estimates of the rate of divergence (d_N/d_S) for autosomal and X-linked genes in (A)**
582 ***P. reticulata*, (B) *P. wingei*, (C) *P. picta*, (D) *P. latipinna* and (E) *G. holbrooki*.** For all species,
583 the X chromosome category excludes genes on the PAR. Additionally, in *P. reticulata* and *P.*
584 *wingei*, the X chromosome category excludes genes in Stratum I. In *P. latipinna* and *G.*
585 *holbrooki*, the X chromosome represents the chromosome syntenic to guppy chromosome
586 12. 95% confidence intervals are based on bootstrapping with 1,000 replicates. Differences
587 between autosomal and X-linked loci are based on 1,000 replicates permutation tests. Only
588 significant differences are shown (p value < 0.01).

589 **Figure 2. Fast-X effect, calculated as the ratio of d_N/d_S for the X chromosome (excluding**
590 **the PAR) to that of the autosomes, across the poeciliids.** In *P. latipinna* and *G. holbrooki*,
591 the X chromosome represents the chromosome syntenic to guppy X. 95% confidence
592 intervals are based on bootstrapping with 1,000 replicates. Green color shading represents
593 the extent of sex chromosome degeneration (mild degeneration in light green to extreme
594 degeneration in dark green), while species in which the guppy chromosome 12 has not been
595 implicated as the sex chromosome are shown in grey.

596 **Figure 3. Estimates of rates of evolution in wild *P. reticulata* populations.** (A) Fast-X effect
597 across *P. reticulata* upstream, low predation populations (orange) and downstream, high
598 predation populations (black) in the Quare, Aripo and Yarra rivers. The Fast-X effect is
599 calculated as the ratio of the rate of nonsynonymous over synonymous substitutions for the
600 X chromosome, excluding the PAR, relative to that for the autosomes.
601

602 **Tables**

603

Table 1. Differences between nonsynonymous and synonymous polymorphisms on the autosomes and X chromosome of each species. For all species, the X chromosome category excludes genes on the PAR.

Species	Category	P_N	P_S	*p* value[a]
P. reticulata	Autosomes	1,890	5,566	*p* = 0.76
	X chromosome	59	184	
P. wingei	Autosomes	650	1,783	*p* = 0.69
	X chromosome	18	56	
P. picta	Autosomes	837	2,178	*p* = 0.24
	X chromosome	12	47	
P. latipinna	Autosomes	1,165	3,265	*p* = 0.24
	Chromosome syntenic to guppy X	52	107	
G. holbrooki	Autosomes	1,212	4270	*p* = 0.08
	Chromosome syntenic to guppy X	28	144	

[a]*p* values from Fisher's Exact test

604

605 **Figures**

606 **Fig. 1**

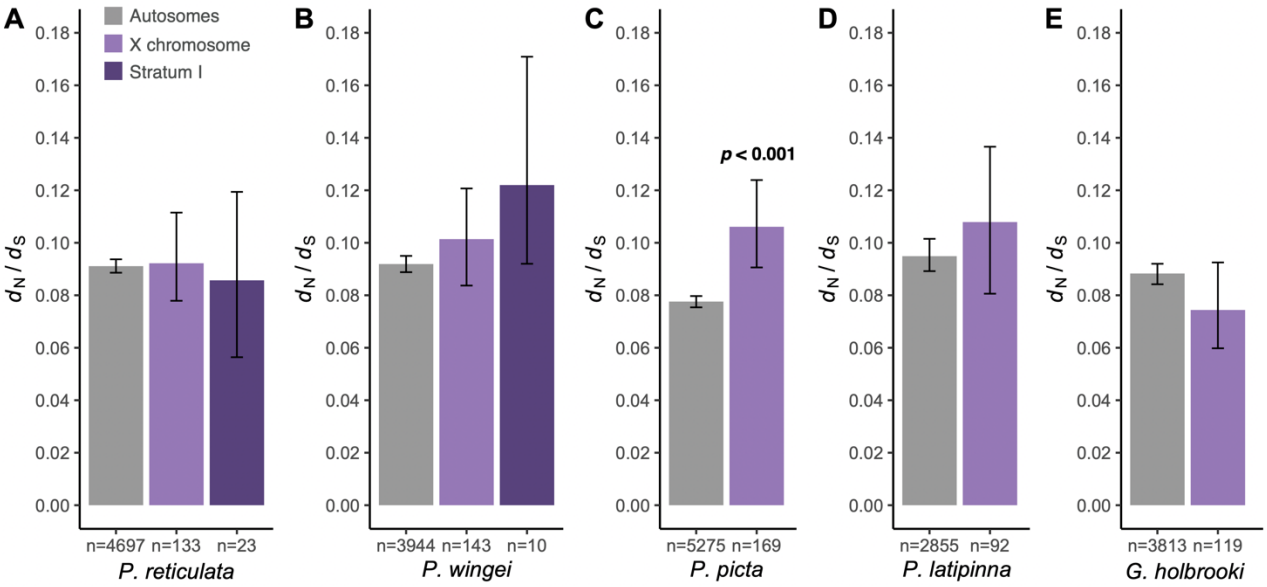

607

608 **Fig. 2**

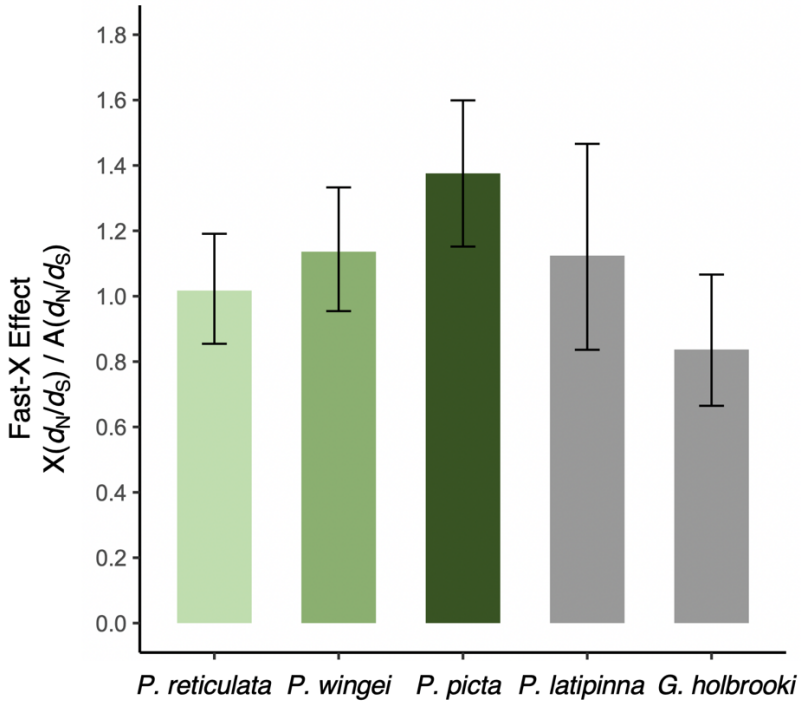
Fast-X Effect
X(d_N/d_S) / A(d_N/d_S)
1.8
1.6
1.4
1.2
1.0
0.8
0.6
0.4
0.2
0.0
P. reticulata
P. wingei
P. picta
P. latipinna
G. holbrooki

609

610 **Fig. 3**

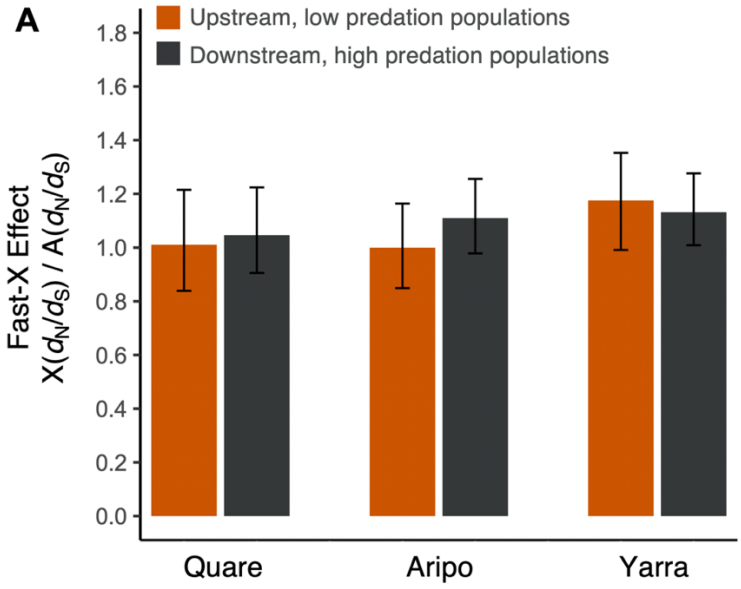
A
Upstream, low predation populations
Downstream, high predation populations
Fast-X Effect
X(d_N/d_S) / A(d_N/d_S)
1.8
1.6
1.4
1.2
1.0
0.8
0.6
0.4
0.2
0.0
Quare
Aripo
Yarra

611